Aerosol and Air Quality Research, 14: 596–607, 2014

ISSN: 1680-8584 print / 2071-1409 online
doi: 10.4209/aaqr.2013.03.0082

Satellite Retrievals of Aerosol Optical Depth over a Subtropical Urban Area: The Role of Stratification and Surface Reflectance

Jerónimo Escribano[1,2*], Laura Gallardo[1,3], Roberto Rondanelli[1,3], Yong-Sang Choi[4]

[1] *Center for Climate and Resilience Research (CR)2, Chile*
[2] *Centro de Modelamiento Matemático, Universidad de Chile (CNRS UMI 2807). Blanco Encalada 2120, Santiago, Chile*
[3] *Departamento de Geofísica, Universidad de Chile. Blanco Encalada 2002, Piso 4, Santiago, Chile*
[4] *Department of Environmental Science and Engineering, Ewha Womans University, Seoul, Korea*

ABSTRACT

We explore the relationship between satellite retrievals of aerosol optical depth (AOD) and surface aerosol mass concentrations over a subtropical urban area, namely, Santiago, Chile (33.5°S, 70.6°W, 500 m.a.s.l.). We compare 11 years of AOD from the MODerate resolution Imaging Spectroradiometer (MODIS) with in situ particulate matter mass concentrations (PM). MODIS AOD reaches its maximum in summer and minimum in winter, the opposite of the annual cycle of surface PM. To improve our understanding of the relevant governing processes, we use a simple model that estimates the boundary layer (BL) AOD based on measured PM, relative humidity and BL height (BLH) as well as best estimates of aerosol composition, size distribution, and optical properties. Model results indicate that a weak annual AOD cycle is due to the opposite annual cycles in BLH and PM, which is largely supported by the Aerosol Robotic NETwork (AERONET) data collected in 2001 and 2002 in Santiago. We identify a possible bias linked to the operational estimate of surface reflectance that may lead to a spurious summer maximum in MODIS AOD over Santiago. This misfit in surface reflectance appears to affect not only Santiago but also a significant area of the semi-arid Southern South America. Sensitivity experiments with the simple model indicate an underestimate of simulated AOD as compared to AERONET data. This underestimate points to the possible role of residual aerosol layers in the AOD measured at the surface (not included in the simple model). Cirrus clouds appear not to play a significant role in explaining the MODIS AOD seasonality. The need for improved characterizations of aerosol properties and their temporal and spatial distribution in cities such as Santiago is emphasized.

Keywords: MODIS; AOD; Surface reflectance; Particulate matter.

INTRODUCTION

Air quality is an issue of concern in many South American cities, and substantial efforts have been made by local authorities to measure so-called criteria pollutants (Gallardo *et al.*, 2012a and references therein). However, aerosol measurements in the region are still sparse and usually limited to mass concentrations of partially (PM_{10}) and completely ($PM_{2.5}$) inhalable particles, which hampers their usefulness as tools for improved understanding of impacts on health, ecosystems and climate, and for the actual evaluation and design of curbing policies. Thus, it is appealing to use remote sensing to supplement existing ground measurements where available or to infer ground concentrations of particles where absent. In fact, if at a given location urban aerosols are the dominant source of atmospheric turbidity, one would expect to find a relationship between aerosol optical depth (AOD or τ) and particulate matter (PM), as reported for many locations (e.g., Engel-Cox *et al.*, 2004; Pelletier *et al.*, 2007; Schaap *et al.*, 2009; Boyouk *et al.*, 2010; Tsai *et al.*, 2011; Estellés *et al.*, 2012). However, such a relationship is modulated by local emissions and meteorological conditions, as well as by the assumptions underlying the retrieval of AOD (e.g., Song *et al.*, 2009). Therefore, validation studies of remotely sensed AOD should consider local conditions and expertise, and provide an explanation of the AOD-PM relationship based on physical principles.

One of the space-borne instruments that acquire AOD is the MODerate resolution Imaging Spectroradiometer (MODIS), which is a 36-band spectrometer widely used by the research community (Kaufman *et al.*, 1997; Remer *et al.*, 2005; Levy *et al.*, 2007a, b; Levy *et al.*, 2009). MODIS AOD has been validated against ground-based AOD

* Corresponding author.
Tel.: 56-2-29784300
E-mail address: jescribano@dim.uchile.cl

measurements collected by the Aerosol Robotic NETwork (AERONET, Holben *et al.*, 1998) for different atmospheric conditions and different locations with encouraging results (e.g., Levy *et al.*, 2010; Bréon *et al.*, 2011; Hyer *et al.*, 2011; Mei *et al.*, 2012).

The MODIS retrieval algorithm for AOD considers assumptions regarding surface reflectance, aerosol properties, etc. (Levy *et al.*, 2007a, b). In particular, surface reflectance estimates are crucial in the AOD retrievals in the case of low aerosol loading over land ($\tau \lesssim 0.15$) (Levy *et al.*, 2010). Recently improved methods for the treatment of surface reflectance have been proposed. For example, He *et al.* (2012) and Guang *et al.* (2012) use a Bidirectional Reflectance Distribution Function (BRDF) model to calculate both the surface reflectance and the MODIS AOD simultaneously. An analysis of the MODIS AOD algorithm sensitivity to the surface reflectance assumptions is presented by Mielonen *et al.* (2011), and modifications to the surface reflectance parameterization of the MODIS AOD algorithm are proposed by Oo *et al.* (2010) and Mielonen *et al.* (2011). Also, it has been shown that the MODIS algorithm is sensitive to thin cirrus contamination (Gao *et al.*, 2002; Roskovensky and Liou, 2005). Moreover, Drury *et al.* (2008), Drury *et al.* (2010), and Schwartz *et al.* (2012) have reported difficulties in MODIS AOD over arid and semi-arid region in the southwestern United States due to a bias in MODIS AOD linked to inaccurate estimations of surface reflectance. In summary, surface reflectance is a key parameter, subject to uncertainties, that must be carefully evaluated to establish the relationship between AOD and PM, particularly over arid and semi-arid zones. Hoelzemann *et al.* (2009) presented a multiyear comparison for South America between ground-based AERONET AOD observations and the MODIS AOD satellite product. This analysis excluded stations in Southern South America (SSA) where only a few places have sunphotometer records for more than two years and therefore compromise the adequate validation of any space-borne instruments that acquire AOD (MODIS in particular) over SSA.

We attempt to investigate the applicability of MODIS AOD to assess the aerosol loading in the boundary layer for Santiago de Chile (33.5°S 70.6°W, 500 m.a.s.l), where health concerns (e.g., Valdés *et al.*, 2012) and potentially cloud and climate impacts (e.g., Saide *et al.*, 2012) require an improved characterization of atmospheric particulates. Moreover, we chose Santiago because it is located under the prevailing subsiding regime imposed by the South Eastern Pacific anticyclone, which contributes to both a well-defined and very stable boundary layer (e.g., Muñoz and Undurraga, 2010; Saide *et al.*, 2011), and a large number of clear days for successful AOD retrievals. Given the heavy load of particulates over Santiago and the absence of frequent visible aerosol layers above the boundary layer, we expected to find a direct relationship between AOD and PM. However, when comparing 11 years of MODIS AOD and concurrent PM surface concentrations, we found that MODIS AOD is at a maximum in summer and minimum in winter, as opposed to the annual cycle of surface PM, shown in Figs. 1(a) and 1(b). This unexpectedly different seasonality should be interpreted only qualitatively since ground-based AOD measurements by an AERONET sunphotometer that are coincident with MODIS (78 days between 2001 and 2002, mostly in summertime) show a systematic upward bias of the MODIS AOD with respect to AERONET AOD, if AERONET data are considered as "truth" (See Fig. 1(c)).

In order to improve our understanding of the relevant governing processes behind the aforementioned AOD-PM relationship, we implemented a simple model that estimates the boundary layer (BL) AOD based on measured PM, relative humidity, and BL height (BLH), as well as best estimates for aerosol composition, size distribution, and optical properties. This simple model was subsequently applied to describe the diurnal variability of AOD, testing simple model results against sunphotometer data collected during a short campaign, and against available AERONET data.

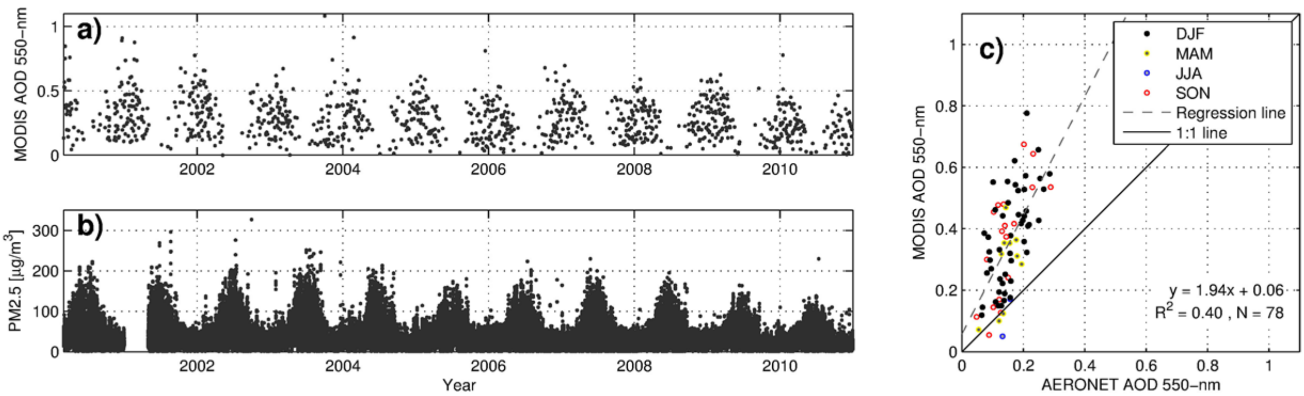

Fig. 1. Time series of MODIS AOD successful retrievals over Santiago (a) and $PM_{2.5}$ hourly measurements in Parque O'Higgins, in downtown Santiago (b), and scatter plot of concurrent MODIS AOD and AERONET AOD (c). The AERONET AOD in panel (c) were calculated using the average of level 2 AERONET AOD over a ± 30 minute window around MODIS pass time and only if 3 or more successful retrievals in the ± 30 minute window were available. For comparison with MODIS AOD, AERONET AOD at 0.55-µm was computed by linear interpolation between 0.5-µm and 0.675-µm on a log-log plot, based on Ångström power law.

Above all, this study explores the physical basis of the AOD-PM relationship, and identifies the potential cause for inconsistency between MODIS and AERONET measurements not only over Santiago, but also possibly over other subtropical areas. We expect that this study can trigger more thorough exploration of boundary layer and aerosol processes in Santiago, based on improved observational platforms that integrate satellite and ground based measurements.

In the following paragraphs we present the data used in this study. The simple model is described thereafter. Results and discussion will follow the model description, and we will close with summary and conclusions.

DATA

Hourly records of particulate matter with aerodynamic diameter less than 10 µm (PM_{10}) and less than 2.5 µm ($PM_{2.5}$) at four stations in Santiago are available from the Ministry of Environment for the 2000–2010 period (http://sinca.mma.gob.cl/). In this study, we used hourly averages of PM_{10} and $PM_{2.5}$ mass concentrations from the Parque O'Higgins station located in downtown Santiago (Fig. 2). For one day in the winter of 2011, we also looked at 5-minute averages of PM_{10} and $PM_{2.5}$ mass concentrations at Parque O'Higgins. We chose this station because it is located in a park in a flat area and reflects average conditions of the basin as shown by Osses *et al.* (2013). They introduced a "representativity" index for a given station that is linked, on the one hand, to the precision of the measurements, and, on the other hand, to the magnitude of the measurements. With respect to the Osses *et al.* (2013) "representativity" index, Parque O'Higgins is a good proxy for average PM conditions in Santiago, confirming the assumption made previously by various authors (e.g., Gallardo *et al.*, 2012a and references therein) of using Parque O'Higgins as a representative site for the average air quality in Santiago.

Composition and, more rarely, size distribution have been assessed sporadically for aerosols in Santiago in connection with short-term campaigns (e.g., Morata *et al.*, 2008; Gramsch *et al.*, 2009). In this study, we used the aerosol composition reported in the latest version of the Attainment Plan for Santiago (PPDA, 2010), which refers to a composition analysis of particulates in Santiago for 2005 which, to the best of our knowledge, has not been published in the scientific literature. The composition adopted here is shown in Table 1. Very recently, Carbone *et al.* (2013) reported results from a few months' record of aerosol composition using an Aerosol Chemical Speciation Monitor. These data suggest a larger fraction of organic aerosols than the one considered in PPDA (2010). Nevertheless, lacking a better characterization of the optical

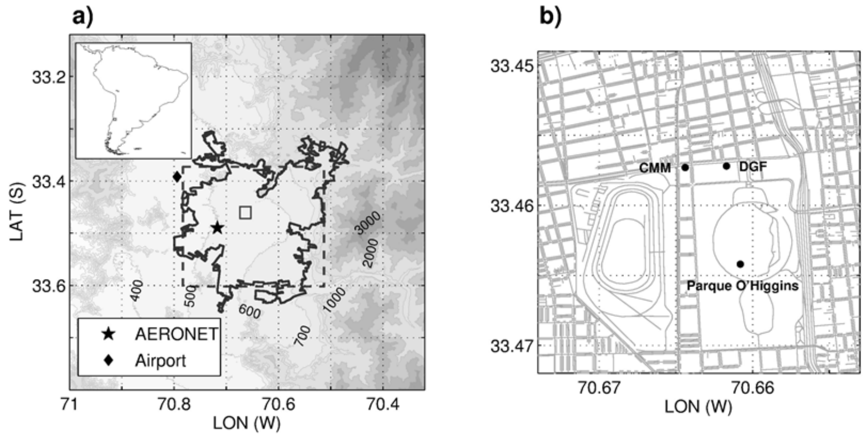

Fig. 2. Santiago de Chile urban area and topography. Measurement sites considered in this study are indicated. The black continuous line in (a) represents the urban area, the dotted rectangle is the 25 km by 25 km square considered for MODIS data. Gray-scale regions, thin gray lines and numbers indicate height above sea level in meters. A detail of the small square is shown in (b). The map data were obtained from http://www.openstreetmap.org.

Table 1. Aerosol composition used in the simple model based on PPDA (2010). Percentages are in terms of total $PM_{10-2.5}$ or $PM_{2.5}$ for each measurement. Complex refractive index (m) and particle density (ρ) are also shown.

Aerosol Type	$PM_{2.5}$ Mass	$PM_{10-2.5}$ Mass	$m = n + ik$	m ref.	ρ [g/cm^3]	ρ ref.
Black Carbon	50%	0%	1.95 + 0.79i	Bond and Bergstrom (2006)	1.8	Bond and Bergstrom (2006)
$(NH_4)_2SO_4$	13.5%	0%	1.53 + 0.006i	Mallet *et al.* (2003)	1.8	Mallet *et al.* (2003)
NH_4NO_3	28.5%	0%	1.56	Global Aerosol Climatology Project	1.7	Gysel *et al.* (2002)
Dust	8%	100%	1.56 + 0.006i	Seinfeld and Pandis (2006)	2.6	see "Data" section

properties, particularly of organic aerosols, we used the 2010 partitioning assuming that all carbonaceous aerosols are as absorbing as black carbon. With lack of better data, aerosol refractive indexes and densities were taken from the literature, except for the density of dust. Morata *et al.* (2008) provided a mineralogical analysis of collected aerosols in Santiago with aerodynamic diameter > 2 µm. These particles can be associated with the dust category in Table 1 (Valdés, 2011). Dust density was estimated by weighting each mineral according to the speciation referred to by Morata *et al.* (2008).

In the early 1990's in Santiago, Horvath and Trier (1993) and Trier and Horvath (1993), reported bulk aerosol extinction coefficients in the range 0.1 to 1, Ångström exponent (~1.22) and aerosol mass extinction coefficients (~5 m^2/g). However, emission patterns in Santiago have changed significantly since this period (e.g., Gallardo *et al.*, 2012b) and, lacking recent data and instead of using results from Horvath and Trier (1993), we use AOD derived from the AERONET record collected in Santiago from August 2001 to October 2002 to compare with our simple model AOD simulations (This model is described later in the paper). The AERONET data set contains ~7800 AOD measurements of Level 2 data and 53 inversions (Dubovik and King, 2000) for aerosol properties (e.g., size distribution, phase function, single scattering albedo) over Santiago. These inversions have an average asymmetry parameter of 0.7 for a 441-nm wavelength and 0.63 for a 675-nm wavelength, with standard deviations of 0.03 and 0.04, respectively. The average Ångström exponent of all measurements between 440 and 675-nm was, 1.3 with a standard deviation of 0.4. Single scattering albedo (ω) was calculated for 10 inversions, resulting in ω ~0.91 at visible wavelengths (standard deviation ~0.05). Both ω and the asymmetry parameters were not used in the model simulation, and they are presented only to note the similarity of the AERONET-derived aerosol optical properties to those used in the moderately absorbing model by the MODIS land algorithm.

Aerosol, land, and cloud products are available from the MODIS Atmosphere group website (http://modis-atmos.gsfc.nasa.gov). Terra and Aqua are polar orbiting satellites with approximate local pass times (UTC-4) of 10:30 and 14:30, respectively, over Santiago. Since BLH data are available for the morning hours as described in Muñoz and Undurraga (2010), we use data collected from the Terra satellite only. Nevertheless, the seasonal behavior of AOD is similar for both platforms over Santiago (not shown). Aerosol products correspond to MOD04 level 2, Collection 5.1. The reliability of the MOD04 product is expressed by a Quality Assurance Confidence (QAC) flag, which varies between 0 ("no confidence") to 3 ("very good confidence") (e.g., Levy *et al.*, 2009; Hubanks *et al.*, 2012). We adopted the recommendation of the MODIS team and used QAC = 3 (Levy *et al.*, 2009), which corresponds to 17% of the pixels over Santiago. Deep Blue products (Hsu *et* al., 2004, 2006) could not be used since 99% of the pixels over Santiago presented QAC flag in the "marginal" or "no confidence" categories. Due to the complex topography surrounding Santiago, we considered a 25 km by 25 km square over the city (Fig. 2) and each daily value of MODIS was calculated as an average of all pixels with QAC = 3 in the 25 km by 25 km square.

Additional sunphotometer data were collected on July 22, 2011 using a Microtops II sunphotometer at the Center for Mathematical Modeling (CMM) building within the Faculty for Physical and Mathematical Science (FCFM, from the Spanish acronym of Facultad de Ciencias Físicas y Matemáticas), University of Chile (Fig. 2).

We took cloud properties retrievals from the MODATML2 Joint Atmosphere products (http://modis-atmos.gsfc.nasa.gov). The MOD43B1 product (Schaaf *et al.*, 2002), which includes the Bidirectional Reflectance Distribution Function (BRDF) model parameters, was used to estimate the surface reflectance in the selected pixels of MOD04. Additionally, we considered cloud observations taken regularly at the Santiago international airport (Fig. 2) by the Chilean Weather Office. This data set includes type of observed cloud, cloud height, and cloud cover in octas.

On the roof of the Department of Geophysics (DGF) at the FCFM in downtown Santiago (Fig. 2), a complete meteorological station and a ceilometer (CL31 Väisälä) have been operational since 2007, allowing a climatology of the BLH (Muñoz and Undurraga, 2010), as well as an indication of aerosol loading (Muñoz and Alcafuz, 2012). These data are used in the simple model described in the next section.

SIMPLE AEROSOL OPTICAL DEPTH MODEL

For simplicity´s sake, we consider an externally mixed aerosol model. Total AOD is the sum of contributions of each aerosol type, which is based on a model shown by Seinfeld and Pandis (2006) as

$$\tau_j = \int_0^{BLH} \int_0^{D_p^{max}} \frac{\pi D_p^2}{4} Q_{ext} n_j \, dD_p dz, \qquad (1)$$

where j identifies each aerosol composition in Table 1; BLH is the boundary layer height; D_p is the particle diameter; D_p^{max} is maximum the particle diameter to be considered in the integration; $Q_{ext}(m,RH,\lambda,D_p)$ is the extinction efficiency; m is the complex refractive index; λ is the wavelength considered; $n_j(D_p, \mathrm{RH}, \mathrm{PM}_{2.5}, \mathrm{PM}_{10})$ is the aerosol number size distribution; RH is the relative humidity.

Dust aerosol number size distribution corresponds to a rural distribution taken from Jaenicke (1993); ammonium nitrate and ammonium sulfate distributions are based on those described by Plaza *et al.* (2011), and the black carbon distribution is a unimodal distribution based on measurements by Gramsch *et al.* (2009). These distributions are numerically represented by more than 40 size bins, and to take into account PM mass concentration observations, these above presented a priori distributions are scaled according to the PM_{10} and $PM_{2.5}$ values such that

$$\int_0^{2.5[\mu m]} n_{m_j}(D_p) dD_p = \mathrm{PM}_{2.5j} \;\; [\mu g/m^3], \qquad (2)$$

and

$$\int_0^{10[\mu m]} n_{m_j}(D_p)dD_p = PM_{10j} \ [\mu g/m^3], \quad (3)$$

where PM_{10j} and $PM_{2.5j}$ are mass concentration of the aerosol type *j* of Table 1. PM_{10j} and $PM_{2.5j}$ values are calculated as the product between the PM_{10} (or $PM_{2.5}$) mass concentration, and the "PM mass" factor shown in Table 1 (e.g., if $PM_{2.5}$ = 40 [μg/m^3], then $PM_{2.5\text{Black Carbon}}$= 40 × 0.5 = 20 [μg/m^3]). Also, in Eqs. (2) and (3), $n_{mj}(\cdot)$ is the mass distribution for composition *j*, calculated on the basis of the number distribution and assuming spherical and constant density particles. The density of the particles depends on the density of the aerosol (Table 1) and is adjusted using density changes due to water uptake for the hydrophilic particles - in this model, ammonium nitrate and sulfate.

Hygroscopicity of ammonium nitrate and ammonium sulfate are taken from Gong *et al.* (2003) and the refractive indexes for the hydrophilic particles are calculated using a simple volume mixing rule as described by Levoni *et al.* (1997). Extinction efficiency is calculated for each aerosol-bin using a Mie scattering calculation code provided by Mätzler (2002).

Lacking a vertical profile for the PM, we assume a well-mixed aerosol profile between the surface and the top of the boundary layer. BLH data are multi-year averages obtained from Muñoz and Undurraga (2010) and adjusted by a simple parameterization of the BLH diurnal cycle. As in the July 22nd case we had ceilometer data, we take advantage of these data assuming a linear relationship between the ceilometer backscattering reflectance and the PM_{10} concentration from the surface to the top of the boundary layer (Muñoz and Alcafuz, 2012).

RESULTS

In this section we show, on the one hand, the ability of our simple model to capture the variability in AOD inferred from sunphotometer measurements. On the other hand, we explore the relationship between MODIS AOD and PM mass concentrations in the boundary layer.

Model Results and Their Validation

Given the many assumptions and uncertainties involved in our simple AOD-PM model, we evaluate its ability to capture the seasonal and diurnal AOD variability. First we examine the ability to capture seasonal variations against available AERONET AOD. In order to verify model runs, we further explore the diurnal variability in AOD by comparing model outputs with AOD data collected by sunphotometer in 2011. Both comparisons also show the model´s sensitivity, respecting the prescribed particle composition and density.

In Fig. 3, seasonal variation of the available AERONET AOD for Santiago (for ca. one year starting in August 2001) at 500-nm wavelength is compared with the model output for our best guess of aerosol composition and density as provided in Table 1. We calculate upper and lower limits for our model outputs considering a range of possible composition and density values. The sensitivity analysis is made with respect to a) variations in particle density, for which we assume ± 25% around the best estimate value, and b) different aerosol compositions, including pure dust, pure ammonium sulfate, pure ammonium nitrate and pure black carbon aerosol. The lower bound of our estimates corresponds to simulations with pure dust and high particle density parameters, while the upper bound corresponds to pure black carbon and low particle density. Each simulation considers the PM and RH values measured within one hour of the AOD observation. AERONET AOD values are generally within the upper and lower bounds of the model uncertainty, and there is qualitative agreement in the seasonal variations of both AOD signals (correlation coefficient of ~0.59 for 12 samples). The largest discrepancies are found in winter (June, July and August) when the least number of observations are available. The modeled AOD values for months with

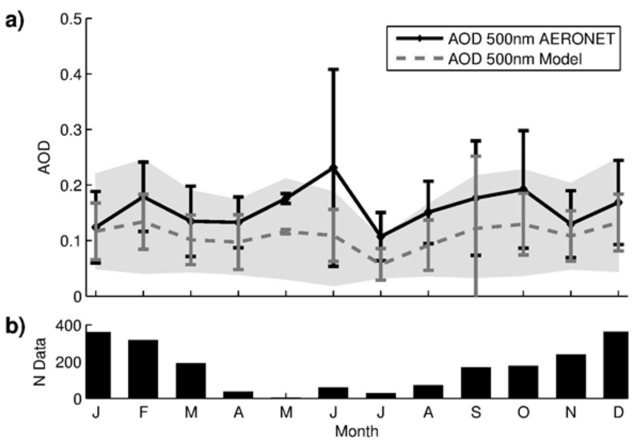

Fig. 3. Monthly means of simulated 500-nm AOD with parameters in Table 1 at AERONET measurement time (gray dotted line) and AERONET 500-nm AOD (black solid line). The bars in (b) represent the total number of AERONET measurements used for each month, and the error bars in (a) the standard deviation. The shaded area around model values represents the sensitivity simulation results at AERONET measurement time (see text for details).

numerous AERONET measurements (September to March) present systematic underestimates, compared to the AERONET AOD.

The exploratory campaign carried out using a Microtops II instrument on the roof of the CMM allows a preliminary evaluation the model with respect to diurnal variations (Fig. 4). No clouds were observed during that day. Evolution of the diurnal BL presents an interesting structure, as shown by the reflectivity of the ceilometer. $PM_{2.5}$ shows a maximum around 12:00 local time, whereas the maximum in AOD occurs two hours later and coincides with a steep increase in BLH from 150–200 m to 350–400 m. Simulated AOD shows a systematic underestimate (~33%), but it captures the variability of the measurements (correlation coefficient ~0.96) in response to the PM vertical profile derived from the ceilometer reflectivity and the PM surface concentration.

In summary, we find that model results show seasonal and single day diurnal variability comparable with that shown in available sunphotometer measurements of AOD. However, a systematic underestimate of simulated AOD values is apparent. Factors such as the existence of internally mixed aerosols (e.g., Jacobson, 2001), non-spherical particles (e.g., Wang *et al.*, 2013) or the presence of upper aerosol layers or residual layers (e.g., Seguel *et al.*, 2013) might help explain model underestimation with respect to observations. The study by Seguel *et al.* (2013) showed near surface ozone origin measured in the residual layer by ozonesondes that accumulates between the top of the mixed layer and the base of the subsidence inversion. Additionally, data from an elastic Light Detection and Ranging system, and a ceilometer over Santiago show unequivocal layers of aerosols above the mixed boundary layer (Muñoz and Alcafuz, 2012). The presence of residual aerosol layers may explain the simple model underestimate of AOD. The contribution of these residual layers of aerosols to total AOD remains as a future question. Despite these shortcomings, we deem the model reliable enough to address seasonal and diurnal variability in AOD. Of course, a more thorough evaluation of the seasonal and diurnal variations in AOD will require more detailed and accurate observations, in particular, systematic and long-term AOD observations over Santiago are required.

MODIS AOD vs. PM Mass Concentrations

Monthly means of MODIS Terra 550-nm AOD retrieval and in situ $PM_{2.5}$ mass concentration measurements at MODIS Terra pass time over Santiago are shown in Fig. 5. Over Santiago, $PM_{2.5}$ concentrations show a strong winter maximum, while MODIS AOD shows a distinct minimum. The depth of the convective boundary layer (BLH) has a strong seasonality at Terra satellite pass time, with ~550 m in summer and ~130 m in winter (Fig. 5). The opposite cycles in BLH (higher in summer and lower in winter) and $PM_{2.5}$ mass concentration (higher in winter and lower in summer) lead to a weak seasonal cycle in the PM burden in our model (not shown). This would result in the weak seasonal cycle of AOD in our model, which is in disagreement to that of MODIS AOD (Fig. 5). To explain this mismatch, we shall check the effects of cirrus contamination and surface reflectance, which seasonal cycles were not considered in our simple model.

To elucidate the effects of cirrus contamination (Gao *et al.*, 2002), we use MODIS cloud related products to check that the pixels used in these comparisons were in fact clear sky in terms of cloud optical depth, cirrus reflectance, and cloud cover fraction. Days with good quality MODIS retrievals were mostly clear-sky (80% clear, 95% partly cloudy with cloud fraction ≤ 0.1; cirrus reflectance < 0.01 in the 99% of the data). Human observers report cloud data at the airport that also corroborate the absence of clouds for most of the MODIS good quality retrievals (72% clear, 85% partly cloudy with cloud fraction ≤ 0.1). One should recognize that human observers might register clouds that are outside the selected satellite pixels over Santiago, and

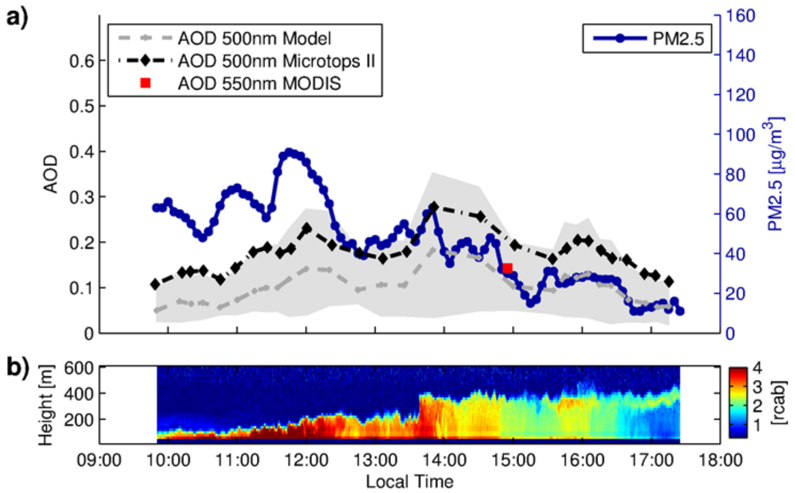

Fig. 4. Short campaign on 22 July 2011. Panel (a) includes simulated 500-nm AOD (gray line), Microtops 500-nm AOD (black line), MODIS Aqua 550-nm AOD (red square) and $PM_{2.5}$ concentrations at Parque O'Higgins station (blue line). The shaded area represents the extent of the sensitivity simulations. Panel (b) includes ceilometer range-corrected attenuated backscatter ([rcab]) in units of $1/(10^6 \cdot \text{srad} \cdot \text{m})$.

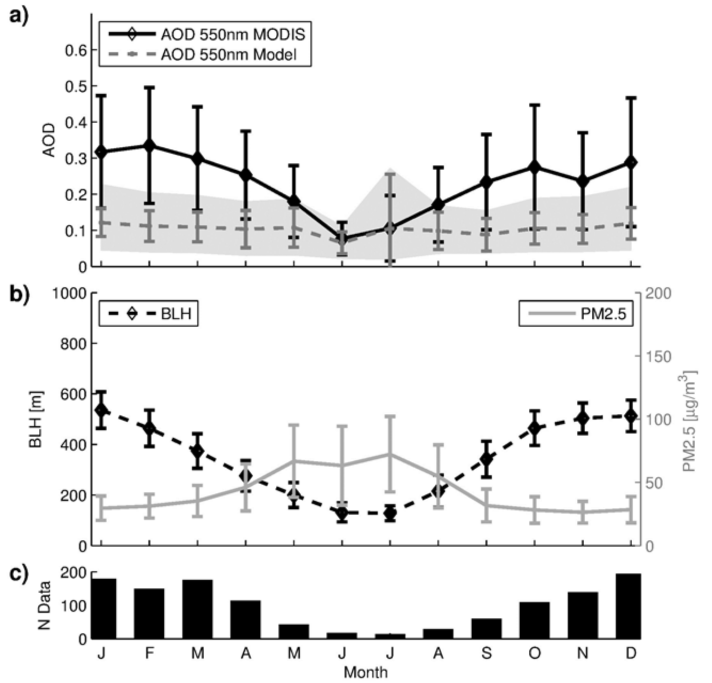

Fig. 5. Panel (a) shows simulated 550-nm AOD at MODIS Terra pass time (gray line) and MODIS Terra 550-nm AOD (black line) monthly means over Santiago. The shaded area represents the extent of the sensitivity simulations at MODIS Terra pass time. The error bars represent standard deviation. Panel (b) presents monthly means of boundary layer height (black line) and $PM_{2.5}$ surface concentration (gray line). Panel (c) shows the total number of MODIS measurements for each month over the entire 2000–2010 period.

these clouds registered by observers might not affect the MODIS retrieval. Also, according to the observers' report, cirrus frequency peaks in spring. Cirrus seasonality is not in phase with the MODIS AOD seasonality, and therefore it can be concluded that cirrus does not explain the MODIS AOD summer maximum.

As stated earlier, surface reflectance is also an important parameter in the MODIS AOD retrieval algorithm. Moreover, MODIS AOD retrievals over places with low AOD ($\tau < 0.15$) are especially sensitive to estimations of surface reflectance (Levy *et al.*, 2010). Santiago is a site with relatively low AOD (Fig. 3) for which an accurate estimate of surface reflectance could be a crucial parameter in MODIS AOD retrieval. The algorithm for MODIS AOD retrieval chooses the best combination of Fine Mode Fraction (η), AOD and surface reflectance such that the difference between observed MODIS reflectance and model-calculated reflectance in the 0.66-µm wavelength is minimized, subject to the constraint that the modeled and observed reflectances in the 0.47 an 2.12-µm channels are equal (Levy *et al.*, 2007a, b; Levy *et al.*, 2009). In order to check the surface reflectance calculations in the aerosol algorithm, we use the combined Terra-Aqua BRDF/albedo level 3 product MCD43 as our surface reflectance guide. The MCD43B1 product includes the parameters of the BRDF model. Re-projecting these data onto a MOD04 grid and using the BRDF algorithm from the Boston University MODIS group (http://www-modis.bu.edu/brdf), we simulate surface reflectance as viewed from the satellite on each pass (Fig. 6). The MODIS AOD operational algorithm has no discernible

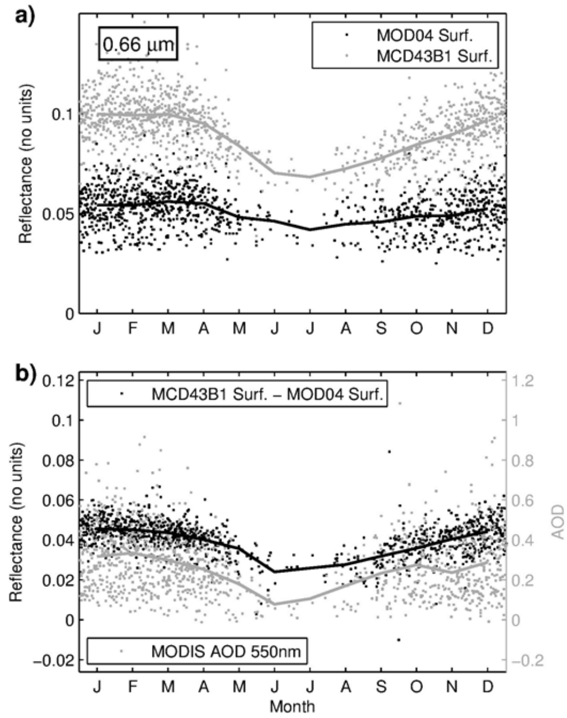

Fig. 6. Panel (a) shows 0.66-µm aerosol algorithm surface reflectance (MOD04, black) and BRDF derived surface reflectance (MCD43B1, gray). Panel (b) presents the difference between the two estimates of surface reflectance (black) and MODIS 550-nm AOD product (gray) over Santiago. Lines show monthly means for retrievals.

seasonal variation in surface reflectance, whereas the BRDF derived product does show a marked seasonal variation in surface reflectance, with higher values in summer (December, January and February). Therefore, the difference between the two surface reflectances presents a seasonal pattern, as do the AOD retrievals (Fig. 6(b)). If we consider surface reflectance from BRDF to be more accurate than surface reflectance from the aerosol algorithm, this difference should be an important source of error when retrieving AOD for Santiago. Moreover, the ratio between 660 nm and 2130 nm BRDF derived surface reflectance (mean of ~0.68 with standard deviation of 0.03) is considerably higher than the MOD04 surface reflectance ratio (mean of ~0.5 with standard deviation of 0.02). Similar differences in the 660/2130 nm ratio of surface reflectance in an urban context have been found by Oo *et al.* (2010) who compare the surface reflectance 600/2130 ratio of the MOD04 algorithm with the one derived from a high spectral resolution Hyperion dataset (Datt *et al.*, 2003).

Finally, aerosol types treated differently would have resulted in the introduction of some biases to AOD. The MOD04 algorithm regards all the pixels analyzed as sulfate aerosol, which is different from the composition reported in Table 1 as well as from the few AERONET inversions that suggest moderately absorbing aerosols. On the other hand, according to the algorithm, 99% of the pixels are tagged as pure coarse mode ($\eta = 0$). This is also different from the mass concentration measurements ratio ($PM_{2.5}/PM_{10} \simeq 0.47$) and/or the $\eta_m = \tau_f/(\tau_f+\tau_c) \simeq 0.8$ indicated by our model, where τ_f and τ_c are the contributions of the fine ($PM_{2.5}$) and coarse ($PM_{10\text{-}2.5}$) aerosols to AOD in the model. The positive difference between real and calculated surface reflectance would lead the algorithm to choose a coarse dust model as the appropriate aerosol model during the minimization of the 0.66-µm channel (Mielonen *et al.*, 2011). Consequently, the surface reflectance products derived from the BRDF and the MOD04 suggest an underestimation of both the magnitude of the surface reflectance at 0.66 µm and the ratio between 660 and 2130 nm surface reflectance. These underestimations lead to the MODIS operational algorithm's election of non-absorbing coarse aerosols over Santiago (e.g., Mielonen *et al.*, 2011), which in turn may result in an overestimate of AOD, particularly in summer when the difference between MOD04 and BRDF surface reflectance estimates is largest.

Other regions in South America could show similar patterns in seasonal differences between the two estimates of surface reflectance and could present similar seasonal behavior in the MODIS AOD retrieval. Maps of seasonal differences between the two estimates of the surface reflectance can be a useful tool to identify these regions, as illustrated in Fig. 7. The amplitude of the seasonal cycle in MODIS AOD, shown in Fig. 7(c), is consistent with the magnitude of the seasonal cycle of the reflectance difference between the two MODIS products (in Fig. 7(f)), especially in the semi-arid Patagonian region in the SSA. A further confirmation that surface reflectance might also be the source of a spurious seasonality is given by AERONET data taken at Trelew (43.3°S, 65.3°W, 15 m.a.s.l). At this site, MODIS AOD shows a summer maximum not observed in the AERONET AOD data (shown in supplementary material). Other cities in SSA that present small differences in the magnitude of surface reflectance, such as Córdoba (31.4°S, 64.2°W) and Buenos Aires (34.6°S, 58.4°W), do not show significant differences in the comparison between MODIS AOD and AERONET AOD seasonality (not shown). Hence, combined evidence strengthens the idea that the MODIS AOD seasonality over Santiago is spuriously driven by the operational estimate of surface reflectance.

SUMMARY AND CONCLUSIONS

In this study, we explored the relationship between MODIS AOD and PM mass concentration over a subtropical urban area in the Southern Hemisphere, namely Santiago de Chile. We applied a simple, semi-empirical AOD-PM model that captures both the diurnal and seasonal variability in AOD according to available sunphotometer measurements. Model results suggest both a weak seasonal variability of AOD over Santiago due to opposite variations in boundary layer height and aerosol mass concentrations and a similar contribution of the $PM_{2.5}$ and BLH variability to the AOD calculation in both diurnal and seasonal time scales. On the other hand, MODIS AOD demonstrates considerable amplitude of the seasonal cycle (~50% below the annual mean in winter and ~20% above the annual mean in summer). Our analysis suggests that cirrus clouds are not the primary reason for the inconsistent seasonality between the MODIS AOD and the simulated AOD. By comparing surface reflectances derived from the operational aerosol algorithm and from the BRDF product, we find that summer reflectances are considerably lower than expected in an urban setting, possibly leading to an overestimate of aerosol AOD. A similar bias in surface reflectance is found over other semi-arid areas of SSA. The simple model suggests that up to one third of the AOD could be attributed to the presence of residual aerosol layers over the estimated BLH. The impact of aerosols within the residual layers in AOD seasonality in both model and observations remains to be quantified.

Our results suggest that the MODIS AOD retrieval algorithm requires an improved estimate of surface reflectance, particularly in summer and over vast semi-arid areas of SSA, and possibly over other arid and semi-arid regions (e.g., Drury *et al.*, 2008). The potential bias in MODIS AOD discussed here over large arid or semi-arid regions could introduce spurious values of AOD in assimilation experiments and potentially affect the determination of aerosol sources, radiative forcing, and air quality calculations (e.g., Huneeus *et al.*, 2012; Saide *et al.*, 2012; Schwartz *et al.*, 2012)

Evidently, there is a need for further validation of satellite borne instruments against in situ measurements and sunphotometers over SSA. Specifically, we expect to reestablish Santiago as an AERONET site. To advance in the quantification of radiative and health related impacts of aerosols over large urban centers in South America will require quality controlled and regular measurements of aerosol composition, size distribution, and optical properties.

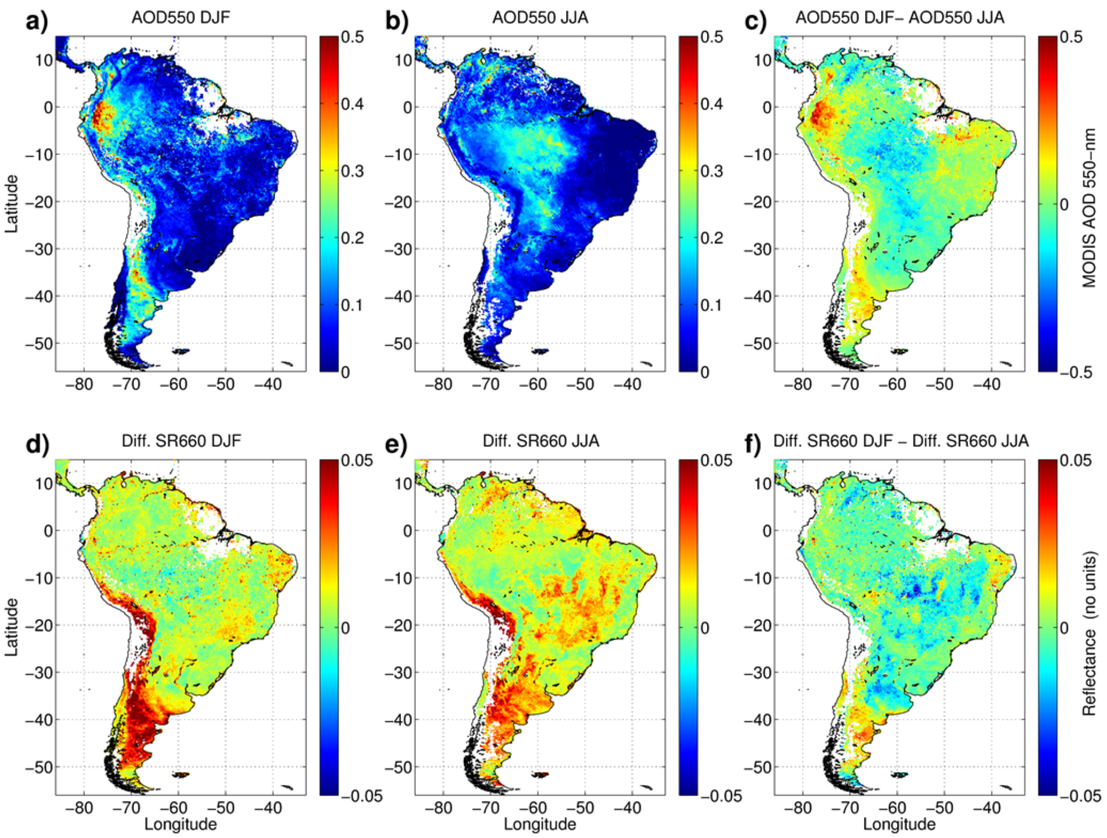

Fig. 7. MODIS derived AOD and differences of between surface reflectance estimates for the MOD04 and the MCD43B1 surface reflectance products for the year 2007. Panel (a) MOD04 AOD in summer, (b): MOD04 AOD in winter, (c): difference between MOD04 AOD in summer and MOD04 AOD in winter, (d): difference between MCD43B1 surface reflectance and MOD04 derived surface reflectance in summer, (e): difference between MCD43B1 surface reflectance and MOD04 derived surface reflectance in winter, (f): difference between panels (d) and (e). The blank regions represent no data. The AOD and surface reflectance are derived from the same data set and using the same data processing as for Santiago MODIS AOD and surface reflectance calculations.

In the case of Santiago where boundary layer processes play such a key role and the presence of not yet characterized residual layers is unequivocal, in situ vertical profiling capabilities must be substantially improved.

ACKNOWLEDGEMENTS

We thank the MODIS and AERONET teams for making their data available. The MICROTOPS II was kindly lent to us by GMAI group at INPE, Brazil. We also acknowledge the Chilean Meteorological Office for cloud observations data. We thank A. Valdés for the estimate of dust density. We appreciate N. Huneeus, F. Mena, K. Indvik and anonymous reviewers for their help in improving this work. J. Escribano acknowledges the fellowship provided by the Center for Mathematical Modeling. This work was carried out with the aid of a grant from the Inter-American Institute for Global Change Research (IAI) CRN II 2017 which is supported by the US National Science Foundation (Grant GEO-0452325), and by Conicyt/FONDAP/15110009, and partially supported by the National Research Foundation of Korea (NRF) grant funded by the Korea government (2009-0083527).

SUPPLEMENTARY MATERIALS

Supplementary data associated with this article can be found in the online version at http://www.aaqr.org.

REFERENCES

Bond, T. and Bergstrom, R. (2006). Light Absorption by Carbonaceous Particles: An Investigative Review. *Aerosol Sci. Technol.* 40: 27–67.

Boyouk, N., Leon, J., Delbarre, H., Podvin, T. and Deroo, C. (2010). Impact of the Mixing Boundary Layer on the Relationship between $PM_{2.5}$ and Aerosol Optical Thickness. *Atmos. Environ.* 44: 271–277.

Bréon, F.M., Vermeulen, A. and Descloitres, J. (2011). An Evaluation of Satellite Aerosol Products Against Sunphotometer Measurements. *Remote Sens. Environ.* 115: 3102–3111.

Carbone, S., Saarikoski, S., Frey, A., Reyes, F., Reyes, P., Castillo, M., Gramsch, E., Oyola, P., Jayne, J., Worsnop, D. and Hillamo, R. (2013). Chemical Characterization of Submicron Aerosol Particles in Santiago de Chile. *Aerosol Air Qual. Res.* 13: 462–473.

Datt, B., McVicar, T., Van Niel, T., Jupp, D., Pearlman, J. (2003). Preprocessing EO-1 Hyperion Hyperspectral Data to Support the Application of Agricultural Indexes. *IEEE Trans. Geosci. Remote Sens.* 41: 1246–1259.

Drury, E., Jacob, D., Wang, J., Spurr, R. and Chance, K. (2008). Improved Algorithm for MODIS Satellite Retrievals of Aerosol Optical Depths over Western North America. *J. Geophys. Res.* 113, D16204.

Drury, E., Jacob, D., Spurr, R., Wang, J., Shinozuka, Y., Anderson, B, Clarke, A, Dibb, J., McNaughton, C. and Weber, R. (2010). Synthesis of Satellite (MODIS), Aircraft (ICARTT), and Surface (IMPROVE, EPA-AQS, AERONET) Aerosol Observations over Eastern North America to Improve MODIS Aerosol Retrievals and Constrain Surface Aerosol Concentrations and Sources. *J. Geophys. Res.* 115: D14204.

Dubovik, O. and King, M. (2000). A Flexible Inversion Algorithm for Retrieval of Aerosol Optical properties from Sun and Sky Radiance Measurements. *J. Geophys. Res.* 105: 20673–20696.

Engel-Cox, J., Holloman, C., Coutant, B. and Hoff, R. (2004). Qualitative and Quantitative Evaluation of MODIS Satellite Sensor Data for Regional and Urban Scale Air Quality. *Atmos. Environ.* 38: 2495–2509.

Estellés, V., Martínez-Lozano, J., Pey, J., Sicard, M., Querol, X., Esteve, A., Utrillas, M., Sorribas, M., Gangoiti, G., Alastuey, A. and Rocadesnbosch, F. (2012). Study of the Correlation between Columnar Aerosol Burden, Suspended matter at Ground and Chemical Components in a Background European Environment. *J. Geophys. Res.* 117: D04201.

Gallardo *et al.*, (2012a). South American megacities in The Impacts of Megacities on Air Quality and Climate Change: An IGAC Perspective, Zhu, T., Parrish, D., Gauss, M., Doherty, S., Lawrence, M., Gallardo, L., Kanakidou, M., Konare, (Eds.), IGAC/WMO Book and Report. Available at http://igacproject.us2.list-manage.com/track/click?u=666486fa44709dd7988985c8d&id=bcdf03a7c8&e=3d15a41ae8 (Accessed in August 2013).

Gallardo, L., Escribano, J., Dawidowski, L., Rojas, N., Andrade, M.F. and Osses, M. (2012b). Evaluation of Vehicle Emission Inventories for Carbon Monoxide and Nitrogen Oxides for Bogotá, Buenos Aires, Santiago and São Paulo. *Atmos. Environ.* 47: 12–19

Gao, B.C., Kaufman, Y.J., Tanré, D. and Li, R.R. (2002). Distinguishing Tropospheric Aerosols from Thin Cirrus Clouds for Improved Aerosol Retrievals Using the Ratio of 1.38-µm and 1.24-µm Channels. *Geophys. Res. Lett.* 29: 1890.

Global Aerosol Climatology Project, Andrew Lacis Database of Aerosol Spectral Refractive Indices, Available at http://gacp.giss.nasa.gov/data_sets/ (Accessed in August 2013).

Gong, S.L., Barrie, L.A., Blanchet, J.P., Salzen, K.V., Lohmann, U., Lesins, G., Spacek, L., Zhang, L.M., Girard, E., Lin, H., Leaitch, R., Leighton, H., Chylek, P. and Huang, P., (2003). Canadian Aerosol Module: A Size-segregated Simulation of Atmospheric Aerosol Processes for Climate and Air Quality Models 1. Module Development. *J. Geophys. Res.* 108: 4007.

Gramsch, E., Gidhagen, L., Wahlin, P., Oyola, P. and Moreno, F. (2009). Predominance of Soot-mode Ultrafine Particles in Santiago de Chile: Possible Sources. *Atmos. Environ.* 43: 2260–2267.

Guang J., Xue, Y., Yingjie, L., Liang, S., Mei, L. and Xu, H. (2012). Retrieval of Aerosol Optical Depth over Bright Land Surfaces by Coupling Bidirectional Reflectance Distribution Function Model and Aerosol Retrieval Model. *Remote Sens. Lett.* 3: 577–584.

Gysel, M., Crosier, J., Topping, D., Whitehead, J., Bower, K., Cubinson, M., Williams, P., Flynn, M., McFiggans, G. and Coe, H. (2007) .Closure Study between Chemical Composition and Hygroscopic Growth of Aerosol Particles during TORCH2. *Atmos. Chem. Phys.* 7: 6131–6144.

He, T., Liang, S., Wang, D., Hongyi, W., Yu, Y. and Wang, J. (2012). Estimation of Surface Albedo and Directional Reflectance from Moderate Imaging Spectroradiometer (MODIS) Observations. *Remote Sens. Environ.* 119: 286–300.

Hoelzemann, J., Longo, K., Fonseca, R., Rósario, N., Elbern, H., Freitas, S. and Pires, C. (2009). Regional representativity of AERONET Observation Sites during the Biomass Burning Season in South America Determined by correlation Studies with MODIS Aerosol Optical Depth. *J. Geophys. Res.* 114: D13.

Holben B.N., Eck, T., Slutsker, I., Tanre, D., Buis, J., Setzer A., Vermote, E., Reagan, J., Kaufman, Y., Nakajima, T., Lavenu, F., Jankowiak, I. and Smirnov, A. (1998). AERONET - A Federated Instrument Network and Data Archive for Aerosol Characterization. *Remote Sens. Environ.* 66: 1–16

Horvath, H. and Trier.A. (1993). A Study of the Aerosol in Santiago de Chile - I. Light Extinction Coefficients. *Atmos. Environ.* 27A: 371–384.

Hsu, C., Tsay, S., King, M. and Herman, J. (2004). Aerosol Properties over Bright-Reflecting Source Regions. *IEEE Trans. Geosci. Remote Sens.* 42: 557–569.

Hsu, C., Tsay, S., King, M. and Herman, J. (2006). Deep Blue Retrievals of Asian Aerosol Properties during ACE-Asia. *IEEE Trans. Geosci. Remote Sens.* 44: 3180–3195.

Hubanks, P. *et al.*, (2012). MODIS Atmosphere QA Plan for Collection 005 and 051, Version 3.10, 12 January 2012. Available at http://modis-atmos.gsfc.nasa.gov/_docs/QA_Plan_2012_01_12.pdf (accessed in August 2013).

Huneeus, N., Chevallier, F. and Boucher, O. (2012). Estimating Aerosol Emissions by Assimilating Observed Aerosol Optical depth in a Global Aerosol Model. *Atmos. Chem. Phys.* 12: 4585–4606.

Hyer, E., Reid, J. and Zhang, J. (2011). An over-land Aerosol Optical Depth Data Set for Data Assimilation by Filtering, Correction and Aggregation of MODIS Collection 5 Optical Depth Retrievals. *Atmos. Meas. Tech.* 4: 379–408.

Jacobson, M. (2001). Strong Radiative Heating due to the Mixing State of Black Carbon in Atmospheric Aerosols. *Nature* 409: 695–697

Jaenicke, R. (1993). Tropospheric Aerosols, In *Aerosol-*

cloud-Climate Interactions, Hobbs, P. (Ed.), Academic Press, San Diego, California, USA.

Kaufman, Y.J., Wald, A., Remer, L., Gao, B.C., Li, R.R. and Flynn, L. (1997). The MODIS 2.1-μm channel - Correlation with Visible Reflectance for Use in Remote Sensing of Aerosol. *IEEE Trans. Geosci. Remote Sens.* 35: 1286–1298.

Levoni, C., Cervino, M., Guzzi, R. and Torricella, F. (1997). Atmospheric Aerosol Optical Properties: A Database of Radiative Characteristics for Different Components and Classes. *Appl. Opt.* 36: 8031–8041.

Levy, R., Remer, L., Mattoo, S., Vermonte, E. and Kaufman, Y. (2007a). Second-generation Operational Algorithm: Retrieval of Aerosol Properties over Land from Inversion of Moderate Resolution Imaging Spectroradiometer Spectral Reflectance. *J. Geophys. Res.* 112.

Levy, R., Remer, L. and Dubovik, O. (2007b). Global Aerosol Optical Properties and Application to Moderate Resolution Imaging Spectroradiometer Aerosol Retrieval over Land. *J. Geophys. Res.* 112.

Levy, R., Remer, L., Tanré D., Mattoo, S. and Kaufman, Y. (2009). Algorithm for Remote Sensing of Tropospheric Aerosol over Dark Targets from MODIS. Collection 005 and 051: Revision 2; Feb 2009, MODIS Algorithm Theorical Basis Document, Available at http://modis-atmos.gsfc.nasa.gov/_docs/ATBD_MOD04_C005_rev2.pdf (Accessed in August 2013).

Levy, R., Remer, L., Kleidman, R., Mattoo, S., Ichoku, C., Kahn, R. and Eck, T. (2010). Global Evaluation of the Collection 5 MODIS Dark-target Aerosol Products over Land. *Atmos. Chem. Phys.* 10: 10399–10420.

Mallet, M., Roger, J., Despiau, S., Dubovik, O. and Putaud, J. (2003). Microphysical and Optical Properties of Aerosol Particles in Urban Zone during ESCOMPTE. *Atmos. Res.* 69: 73–97.

Mätzler, C. (2002). MATLAB Functions for Mie Scattering and Absorption, Research Report No. 2002-08, Institut für Angewandte Physik, Bern, Switzerland.

Mei, L., Xue, Y., Xu, H., Guang, J., Li, Y., Wang, Y., Ai, J., Jiang, S. and He, X. (2012).Validation and Analysis of Aerosol Optical Thickness Retrieval over Land. *Int. J. Remote Sens.* 33: 781–803.

Mielonen, T., Levy, R., Aaltonen, V., Leeuw, G., Huttunen, J., Lihavainen, H., Kolmonen, P., Lehtinen, K. and Arola, A., (2011). Evaluating the Assumptions of Surface Reflectance and Aerosol Type Selection within the MODIS Aerosol Retrieval over Land: The Problem of Dust Type Selection. *Atmos. Meas. Tech.* 4: 201–214.

Morata, D., Polvé, M., Valdés, A., Belmar, M., Dinator, M.I., Silva, M., Leiva, M., Aigouy, T. and Morales, J.R. (2008). Characterization of Aerosol from Santiago, Chile: An Integrated PIXE-SEM-EDX Study. *Environ. Geol.* 56: 81–95.

Muñoz, R. and Undurraga, A. (2010). Daytime Mixed Layer over the Santiago Basin: Description of Two Years of Observations with a Lidar Ceilometer. *J. Appl. Meteorol. Climatol.* 49: 1728–1741.

Muñoz, R. and Alcafuz, R. (2012). Variability of Urban Aerosols over Santiago, Chile: Comparison of Surface PM_{10} Concentrations and Remote Sensing with Ceilometer and Lidar. *Aerosol Air Qual. Res.* 12: 8–19.

Oo, M., Jerg, M., Hernandez, E., Picón, A., Gross, B., Moshary, F. and Ahmed, S. (2010). Improved MODIS Aerosol Retrieval Using Modified VIS/SWIR Surface Albedo Ratio Over Urban Scenes. *IEEE Trans. Geosci. Remote Sens.* 48: 983–1000.

Osses, A., Gallardo, L. and Faúndez, T. (2013). Combining Statistical Information Tools for the Analysis of Air Quality Monitoring Networks. *Tellus Ser. B 65:* 19822.

Pelletier, B., Santer, R. and Vidot, J. (2007). Retrieving of Particulate Matter from Optical Measurements: A Semiparametric Approach. *J. Geophys. Res.* 112.

Plaza, J., Pujadas, M., Gómez-Moreno, F.J., Sánchez, M. and Artíñano, B. (2011). Mass Size Distributions of Soluble Sulfate, Nitrate and Ammonium in the Madrid Urban aerosol. *Atmos. Environ.* 45: 4966–4976.

PPDA (2010). Revisa, Reformula y Actualiza Plan de Prev ención y Descontaminación Atmosférica para la Región Metropolitana (PPDA) (In Spanish), Available at http://w ww.sinia.cl/1292/articles-39262_ppda_stgo.pdf (Access ed in August 2013).

Remer, L., Kaufman, Y., Tanré, D., Mattoo, S., Chu, D., Martins, J., Li, R., Ichoku, C., Levy, R., Kleidman, R., Eck, T., Vermote, E. and Holben, B. (2005). The MODIS Aerosol Algorithm, Products and Validation. *J. Atmos. Sci.* 62: 947–973.

Roskovensky J., and Liou, K., (2005). Simultaneous Determination of Aerosol and Thin Cirrus optical Depths over Oceans from MODIS Data: Some Case Studies. *J. Atmos. Sci.* 63: 2307–2323.

Saide, P., Carmichael, G., Spak, S., Gallardo, L., Osses, A., Mena, M., and Pagowski, M. (2011). Forecasting Urban PM_{10} and $PM_{2.5}$ Pollution Episodes in very Stable Nocturnal Conditions and Complex Terrain Using WRF-Chem CO Tracer Model. *Atmos. Environ.* 45: 2769–2780.

Saide, P., Carmichael, G., Spak, S., Minnis, P. and Ayers, K. (2012). Improving Aerosol Distributions below Clouds by Assimilating Satellite-retrieved Cloud Droplet Number. *PNAS* 109: 11939–11943.

Schaaf, C., Gao, F., Strahler, A., Lucht, W., Li, X., Tsang, T., Strugnell, N., Zhang, X., Jin, Y., Muller, J.P., Lewis, P., Barnsley, M., Hobson, P., Disney, M., Roberts, G., Dunderdale, M., Doll, C., D'Entremont, R., Hu, B., Liang, S., Privette, J. and Roy, D. (2002). First operational BRDF, Albedo Nadir Reflectance Products from MODIS. *Remote Sens. Environ.* 83: 135–148.

Schaap, M., Apituley, A., Timmermans, R.M.A., Koelemeijer, R.B.A. and de Leeuw, G. (2009). Exploring the Relation between Aerosol Optical Depth and $PM_{2.5}$ at Cabauw, the Netherlands. *Atmos. Chem. Phys.* 9: 909–925.

Schwartz, C., Liu, Z., Lin, H.C. and McKeen, S. (2012). Simultaneous Three-dimensional Variational Assimilation of Surface Fine Particulate Matter and MODIS Aerosol Optical Depth. *J. Geophys. Res.* 117: D13202.

Seguel, R., Mancilla, C., Rondanelli, R., Leiva, M. and Morales, R (2013). Ozone Distribution in the Lower Troposphere over Complex Terrain in Central Chile. *J.*

Geophys. Res. 118: 2966–2980.

Seinfeld, J. and Pandis, S. (2006). *Atmospheric Chemistry and Physics: From Air Pollution to Climate Change* (2nd ed.), John Wiley & Sons, Hoboken, New Jersey, USA.

Song, C.K., Ho, C.H., Park, R.J., Choi, Y.S., Kim, J., Gong, D.Y. and Lee,Y.B. (2009). Spatial and Seasonal Variations of Surface PM_{10} Concentration and MODIS Aerosol Optical Depth over China. *Asia-Pac. J. Atmos. Sci.* 45: 33–43.

Trier, A. and Horvath, H. (1993). A Study of the Aerosol in Santiago de Chile II. Mass Extinction Coefficients, Visibility and Ångström Exponents. *Atmos. Environ.* 27A: 385–395.

Tsai, Y., Jeng, Y., Chu, A., Chen, J. and Chang, S. (2011). Analysis of the Relationship between MODIS Aerosol Optical Depth and Particulate Matter from 2006 to 2008. *Atmos. Environ.* 45: 4777–4788.

Valdés, A. (2011). Mineralogie et Geochimie du Materiel Particulaire Respirable (PM_{10} et $PM_{2.5}$) Present Dansl'Air de Santiago, Chili; Contribution à sa caractérisation et l'identification de ses Sources (In French), Doctoral thesis, Université Toulouse III – Paul Sabatier, 236pp. Available at http://thesesups.ups-tlse.fr/1421/ (Accessed in August 2013).

Valdés, A., Zanobetti, A., Halonen, J., Cifuentes, L., Morata, D. and Schwartz, J. (2012). Elemental Concentrations of Ambient Particles and Cause Specific Mortality in Santiago, Chile: A Time Series Study. *Environ. Health* 11: 82.

Wang, Z., Zhang, H., Jing, X., and Wei, X. (2013). Effect of Non-spherical Dust Aerosol on Its Direct Radiative Forcing. *Atmos. Res.* 120–121: 112–126.

Received for review, March 14, 2013
Accepted, October 15, 2013

Supplementary Materials

Supplementary Figure 1: Panels (a) and (b) show available Level 2 AERONET 500-nm AOD time series over Santiago. Panel (a) is displayed on an equivalent temporal scale to that of Figure 1 (a) in the manuscript. Panel (b) displays the same data set with greater temporal resolution. Panel (c): scatter plot of hourly $PM_{2.5}$ surface concentrations and concurrent AERONET 500-nm AOD over Santiago disaggregated by season. The AERONET AOD in panel (c) were calculated using the average of Level 2 AERONET AOD over a ± 30 minute window around PM measurement time and only if 3 or more successful retrievals in the ± 30 minute window were available. Panel (d): Hourly $PM_{2.5}$ surface concentrations and concurrent MODIS 550-nm AOD over Santiago, disaggregated by season.

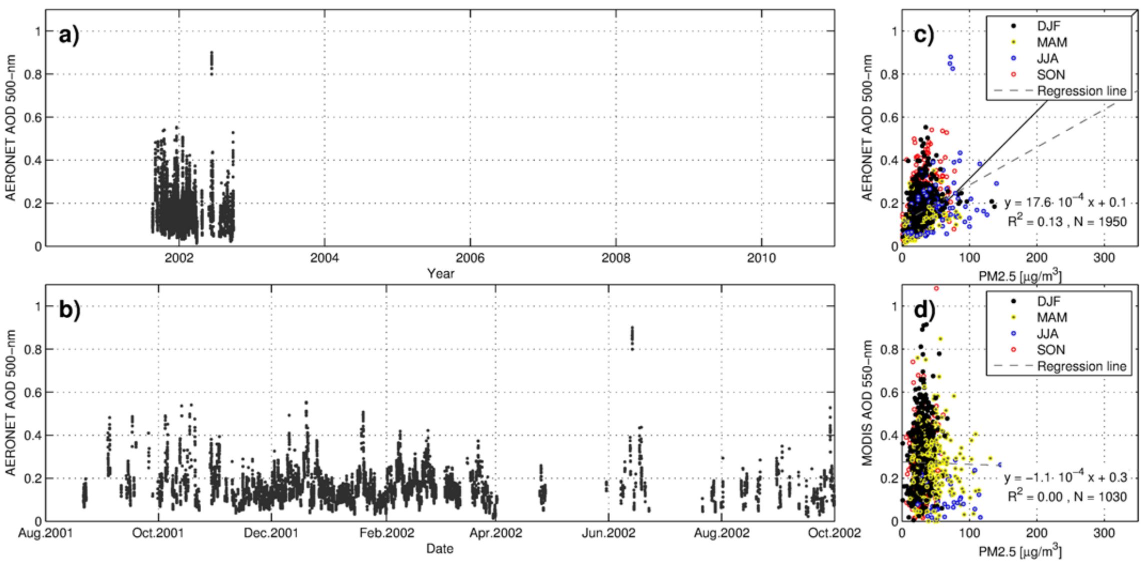

Supplementary Figure 2: Monthly means of AOD and surface reflectance at the Trelew AERONET site for the year 2007. The AOD and surface reflectance belong to the same data set and underwent the same data processing as the Santiago MODIS AOD and surface reflectance. For details please see the main text.